Mono-oxo molybdenum(VI) and tungsten(VI) complexes bearing chelating aryloxides: synthesis, structure and ring opening polymerization of cyclic esters.

Ziyue Sun,[a] Yanxia Zhao,[a*] Timothy J. Prior,[b] Mark R. J. Elsegood,[c] Kuiyuan Wang,[b] Tian Xing[b] and Carl Redshaw[a,b*]

[a] *College of Chemistry and Material Science, Northwest University, 710069 Xi'an, China*

[b] *Department of Chemistry, The University of Hull, Cottingham Rd, Hull, HU6 7RX, U.K.*

[c] *Chemistry Department, Loughborough University, Loughborough, Leicestershire, LE11 3TU, U.K.*

Abstract: The mono-oxo aryloxide complexes $[M(O)(L^1)_2]$ (M = Mo (**1**·hexane), W(**2**·2MeCN)) have been prepared from $[Mo(O)(Cl)_4]$ or $[W(O)(O\textit{t}\text{-Bu})_4]$ and two equivalents of the di-phenol 2,2′-ethylidenebis(4,6-di-*tert*-butylphenol) L^1H_2, respectively. Use of *in-situ* generated $[Mo(O)(O\textit{t}\text{-Bu})_4]$ with two equivalents of L^1H_2 also led to the isolation of **1**·2MeCN. In the presence of adventitious oxygen, attempts to generate *in-situ* $[Mo(O)(O\textit{t}\text{-Bu})_4]$ and reaction with one equivalent of L^1H_2 afforded the bi-metallic complex $[Mo(O)(L^1)(\mu\text{-}O)Li(THF)(MeCN)]_2\cdot 2MeCN$ (**3**·2MeCN). Use of the tetra-phenol α,α,α′,α′-tetrakis(3,5-di-*tert*-butyl-2-hydroxyphenyl)-*p*-xyleneH$_4$ (L^2H_4) with $[Mo(O)(O\textit{i}\text{-Pr})_4]$ led to the isolation of $\{[Mo(O)]L^2\}_2$ (**4**), whilst the analogous tungsten complex $\{[W(O)]L^2\}_2$ (**5**) was isolated from the reaction of L^2H_4 with $[W(O)(O\textit{t}\text{-Bu})_4]$. Similar reaction of p-*tert*-butylcalix[4]areneH$_4$ (L^3H_4) with $[Mo(O)(O\textit{i}\text{-Pr})_4]$ afforded $([Mo(O)L^3(NCMe)]\cdot 3MeCN$ (**6**). Modification of known routes were employed to access the

complexes $[W(Cl)_2L^3]\cdot 3.5MeCN$ (**7**·3.5MeCN) and ($[W(O)L^3(NCMe)]$) (**8**), whilst use of $[WO(Ot\text{-}Bu)_4]$ with L^3H_4 unexpectedly afforded $[W(Ot\text{-}Bu)_2L^3]\cdot MeCN$ (**9**·MeCN). The molecular crystal structures for **1** – **9** are reported, and the ability of these complexes to act as catalysts for the ring opening polymerization (ROP) of ε-caprolactone (ε-CL), δ-valerolactone (δ-VL) and ω-pentadecalactone (ω-PDL) has been investigated. The molybdenum complexes **1** and **4** were the best performers for ε-Cl and δ-VL, but all complexes exhibited poor control and were also inactive toward the ROP of PDL.

Introduction

There has been interest in the coordination chemistry of oxo molybdenum and tungsten species for many years given their relevance to a number of enzyme structures. For example, in the molybdenum oxotransferases, which, as the name suggests, promote oxygen atom transfer reactions, the active site has been identified as containing a mono-nuclear metal centre bound by one or two oxygen centres. [1] Furthermore, there is a drive to model the active site of molybdenum hydroxylase enzymes. [2] Most work has featured *cis*-dioxo molybdenum cores, [3] but a number of mono-oxo systems have been isolated and structurally characterized. [4] Our interest in such species stems from their catalytic potential in polymerization processes, and our on-going investigations into constrained ligand-metal environments. [5] In this context, we have previously screened a small number of molybdenum and tungsten compounds in the ring opening polymerization (ROP) of cyclic esters, [6] and some interesting results were observed for tungsto-systems derived from p-*tert*-butylcalix[*n*]arenes. In particular, for the system based on n = 8, moderate activities were achieved at high temperatures, whereas related n = 6 systems were inactive. [6a] Given this, we have broadened our studies to include a number of oxo species of molybdenum and tungsten, all of which are bound by chelating aryloxide ligands derived from phenols of the type 2,2′-ethylidenebis(4,6-di-*tert*-butylphenol) (L^1H_2), α,α,α′,α′-tetrakis(3,5-di-*tert*-butyl-2-hydroxyphenyl)-*p*-xyleneH$_4$ (L^2H_4) or p-*tert*-butylcalix[4]areneH$_4$ (L^3H_4) (see scheme 1).

In terms of previous work on Mo or W complexes of L^1H_2 or related species, dinuclear (d^3-d^3) species and complexes where the CHR bridge (R = S, Te) in the diphenol have been reported; the latter were

screened in the ROP of norbornene. [7] We have also reported a number of tungsten(IV, VI) halide complexes. [8] For L^2H_4, to the best of our knowledge, there are no reported group 6 complexes, although there have been some recent reports of coordination chemistry and/or catalysis employing other metals. [9] In contrast, there has been considerable work on Mo/W systems derived from L^3H_4 or related compounds. In particular, for metal oxo complexes, Floriani reported the reaction of $[Mo(O)Cl_4]$ with L^3H_4 isolating a complex also containing 'free' L^3H_4 and trapped nitrobenzene. [10] Use of $[W(O)Cl_4]$ led to the structural characterization of the acetic acid solvate of $[W(O)L^3]$ and the benzene solvate of $[W(Cl)_2L^3]$, the latter could be assembled into a supramolecular structure on reaction with sodium phenolate or catecholate. [11a,b] Later, Chisholm *et al* reacted the triply bonded species $Mo_2(L^3H)_2$ with excess O_2 to afford $[Mo(O)L^3]$, [12] whilst Hanna *et al* reported the structure of the benzene solvate $[Mo(O)de\text{-}BuL^3]\cdot C_6H_6$ (where de-BuL^3 = calix[4]arene), which was prepared via the use of LiO*t*-Bu/$[Mo(O)_2Cl_2]$. [13] Harvey and co-workers have reported water/toluene, toluene, and acetonitrile solvates of debutylated L^3 tungsten complexes $[W(O)de\text{-}BuL^3]$, [14a] whilst Brown and Jablonski reported $[W(Cl)_2L^3]$ as a by-product in the formation of a tungstocalix[4]arene phenylimido complex. [14b] An oxotungsten inclusion complex with acetonitrile was also structurally characterized by Pochini and Ugozzoli *et al* for which the *para* substituent on L^3 was cyclohexyl. [15] Herein, the study is focussed on the use of chelating phenoxide ligation at the oxo metal core (see scheme 1), and the similarities in the coordination environments provided by L^1H_2, L^2H_4, and L^3H_4. Additionally, we have examined the use of such species in the ring opening polymerization (ROP) of the cyclic esters ε-caprolactone (CL), δ-valerolactone (δ-VL) and ω-pentadecalactone (PDL).

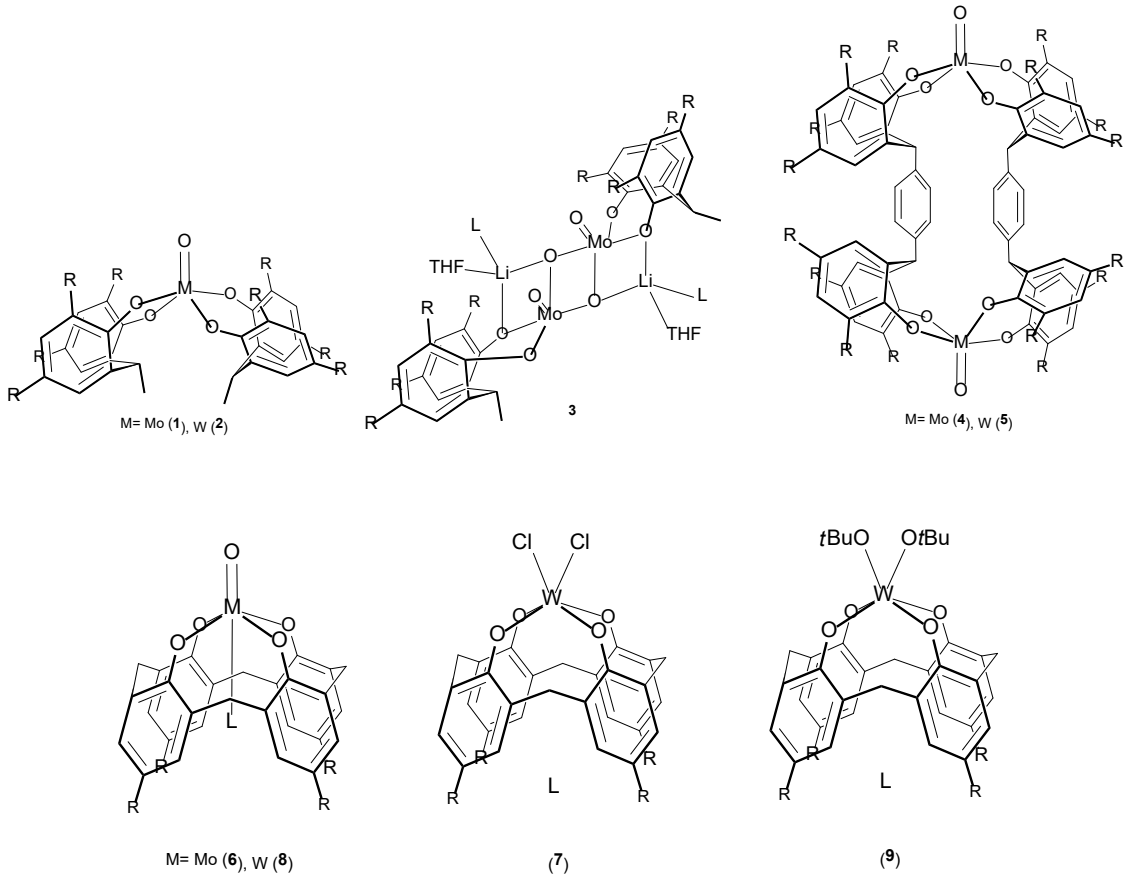

Scheme 1. Complexes **1** – **9** prepared herein (L = MeCN, R = *t*Bu).

Results and Discussion:

Synthesis and molecular structures

Di-phenolates: Reaction of two equivalents of 2,2′-CH(Me)[4,6-(*t*-Bu)$_2$C$_6$H$_2$OLi]$_2$ (L^1Li_2) with [Mo(O)Cl$_4$] afforded, following work-up, the blue complex [Mo(O)L^1_2] (**1**). Stoichiometrically, **1** is formed via loss of four equivalents of LiCl. In the IR of **1**, there is a strong *ν*Mo=O stretch at 963 cm^{-1}. Crystallization from a saturated hexane solution at 0 ºC afforded crystals suitable for an X-ray diffraction study. The molecular structure of **1**·hexane are given in Figure 1, with selected bond lengths and angles in the caption. The complex [Mo(O)$(L^1)_2$] is located on a two-fold axis, with the geometry at the molybdenum best described as distorted trigonal bipyramidal with the phenoxy atoms O(2) and O(2A) axial [O(2)–Mo(1)–O(2A) = 167.81(7)º]. The Mo=O distance [1.6793(16) Å] and Mo–O distances [1.8820(11) – 1.9286(11) Å] are typical of those previously observed for molybdenum(VI) oxo groups and aryloxides respectively. [12-16] Each chelate forms an 8-membered metallocycle with a bite angle of 88.99(5)º and adopting a boat

conformation. The hexane molecule is disordered over a symmetry element. **1** could also be crystallised from acetonitrile to yield **1**·2MeCN which is isostructural with **2**·2MeCN (*vide infra*), see Table 4 for crystallographic data. In the IR of **1**·2MeCN, there is a weak *ν*CN stretch at 2251 cm^{-1}.

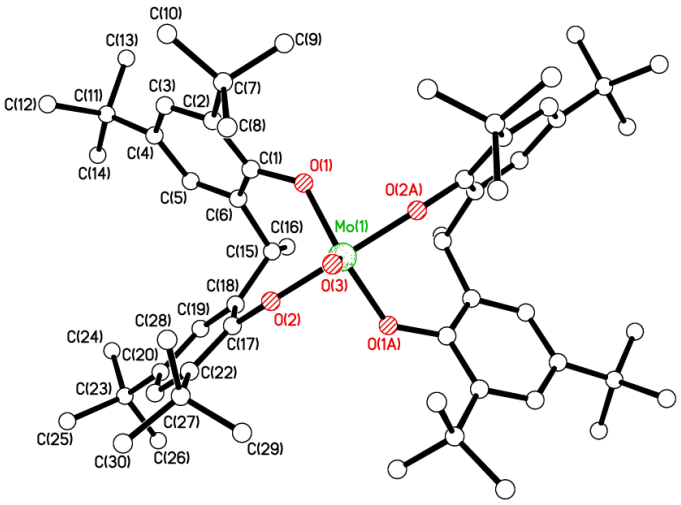

Figure 1. The molecular structure of **1**·hexane viewed approx. parallel to the Mo=O bond. Selected bond lengths (Å) and angles (°): Mo(1)–O(1) 1.9286(11), Mo(1)–O(2) 1.8820(11), Mo(1)–O(3) 1.6793(16); O(1)–Mo(1)–O(2) 88.99(5), O(1)–Mo(1)–O(3) 110.62(3).

In the case of tungsten, the precursor of choice was found to be [W(O)(O*t*-Bu)$_4$] [17] which, upon reaction with L^1H_2 and extraction into acetonitrile, afforded large orange crystals of [W(O)(L^1)$_2$]·2MeCN (**2**·2MeCN) in moderate isolated yield (*ca*. 35 %). While this structure is almost isomorphous with that of **1**·hexane, the space groups are different. The molecular structure of **2**·2MeCN is shown in Figure 2, with selected bond lengths and angles given in the caption. As for **1**, the metal adopts a trigonal bipyramidal geometry with O(2)/O(4) axial. The angles between the planes are C(1) > C(6) *vs* C(17) > C(22) = 87.44(6)° and C(31) > C(36) *vs* C(47) > C(52) = 86.28(6)°. There are also two molecules of acetonitrile in the asymmetric unit, which were both modelled as fully 2-fold disordered. The solvent molecules reside in clefts between the molecules. The packing is such that the metal complexes are arranged in layers with molecules in one column parallel to *a* all having the same orientation, but the next column being inverted relative to the first (see Figure 3). This alternation then continues, and is reminiscent of the structure of p-*tert*-butylcalix[4]areneH$_4$ (L^3H_4) and its solvates. [18]

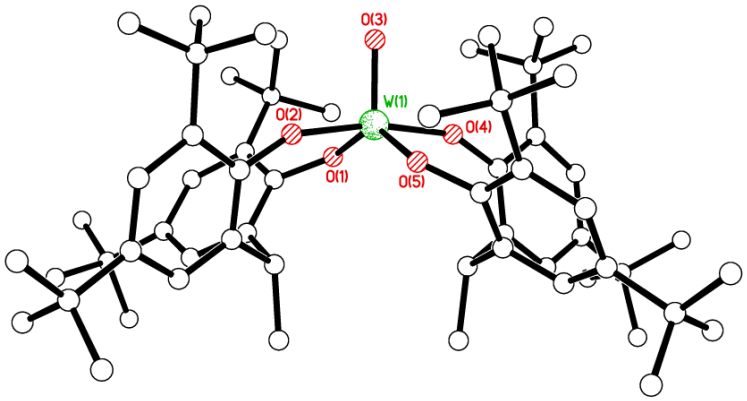

Figure 2. Side view of the molecular structure of **2**·2MeCN. Selected bond lengths (Å) and angles (°): W(1)–O(1) 1.9138(13), W(1)–O(2) 1.8684(13), W(1)–O(3) 1.7037(14), W(1)–O(4) 1.8735(14), W(1)–O(5) 1.9165(13); O(1)–W(1)–O(2) 88.61(6), O(1)–W(1)–O(3) 111.16(3), O(4)–W(1)–O(5) 88.85(6).

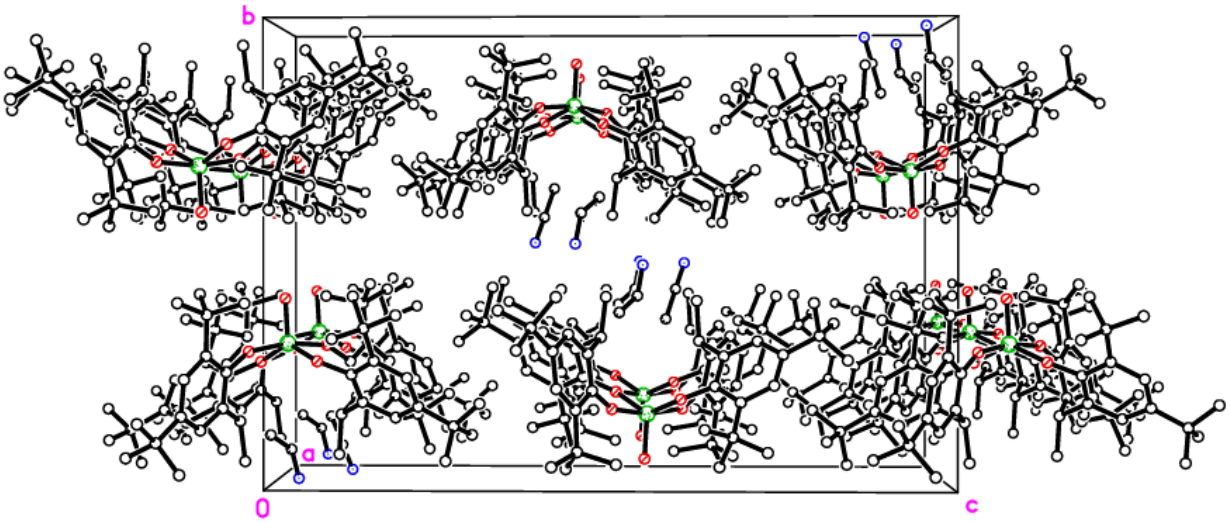

Figure 3. Packing in the crystal structure of **2**·2MeCN.

Attempts to generate *in-situ* [Mo(O)(O*t*-Bu)$_4$] (generated from Mo(O)Cl$_4$ and a slight excess of LiO*t*-Bu (*ie* 4.1 equiv.) and subsequent reaction with one equivalent of L^1H_2, in the presence of adventious oxygen, led to the isolation of the orange/brown complex [Mo(O)(L^1)(μ-O)Li(THF)(MeCN)]$_2$·2MeCN (**3**·2MeCN) in good yield. Single prismatic crystals were grown from a saturated acetonitrile solution at room temperature. The molecular structure of **3**·2MeCN is shown in Figure 4, with selected bond lengths and angles given in the caption. Half of this is the asymmetric unit, so the molecule lies on a 2-fold axis. The absolute structure has been reliably determined for this structure that crystallised in a Sohncke space

group. The core structure comprises a $Mo_2Li_2O_4$ ladder, in which each bisphenolate chelates to a square pyramidal Mo centre and one O also links to a Li. Each Li also coordinates to MeCN and THF as well as a phenolate O atom. The fold angle of the bisphenolate ligand is 82.22(13)°. The ^{1}H NMR spectrum of **3** is broad, consistent with the presence of Mo(V) oxidation states.

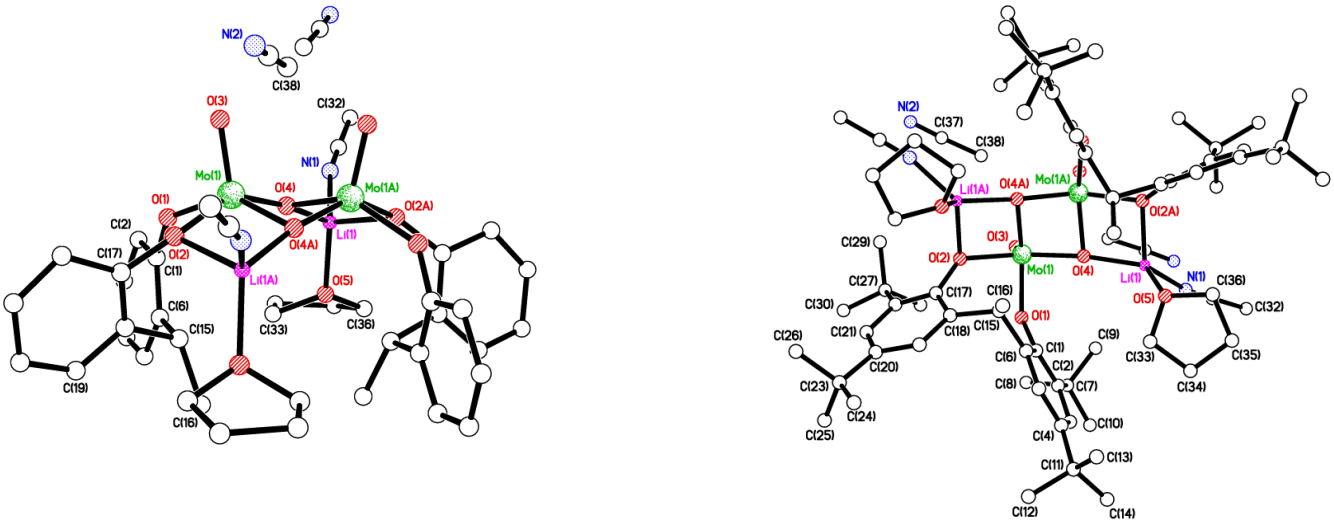

Figure 4. Two views of the molecular structure of **3**·2MeCN. Selected bond lengths (Å) and angles (°): Mo(1)–O(1) 1.962(3), Mo(1)–O(2) 2.027(3), Mo(1)–O(3) 1.670(3), Mo(1)–O(4) 1.945(3), Li(1)–O(2A) 1.977(9), Li(1)–O(4) 1.935(8), Li(1)–O(5) 1.938(9), Li(1)–N(1) 2.039(9), Mo(1)···Mo(1A) 2.6178(7); O(1)–Mo(1)–O(2) 84.02(12), O(2)–Mo(1)–O(4) 147.25(12). Symm. code A = –x+1, –y+1, z.

In the packing, the MeCNs of crystallisation lie close to the Mo=O atoms and the methyl group makes a short contact to this oxygen. Molecules form ABAB layers in the *b*/*c* plane with molecules pointing in opposite directions in the two layers.

Tetra-phenolates: In the case of molybdenum, the reaction of [Mo(O)(O*i*-Pr)$_4$] [19] with the phenol α,α,α′,α′-tetrakis(3,5-di-*tert*-butyl-2-hydroxyphenyl)-*p*-xylene (L^2H_4) resulted, after work-up, in a red/brown complex **4**. Single crystals of **4** suitable for an X-ray structure determination were grown from a saturated hexane solution at 0 °C. The molecular structure of **4** is shown in Figure 5, with selected bond lengths and angles given in the caption. Each molybdenum centre in **4** adopts a distorted trigonal bipyramidal geometry, with the oxo group in the equatorial plane and pointing outwards. The metal centres are linked via two deprotonated L^2 ligands and form a 26-membered metallocycle. The distance between the two Mo centres is 11.428 Å while the separation between

the two central, approximately parallel C_6H_4 rings is *ca*. 3.7 Å This latter separation indicates a weak π···π stacking interaction.

Two 8-membered metallocycles are formed at each end of the complex by the tetra-phenolates, with each adopting a boat conformation. The bite angles of the chelates are in the range 85.8(3) – 89.9(3)º, which is similar than that found (88.99(5)º) in the mononuclear molybdenum complex **1**, but much smaller than that observed for the bis(imido) complex [Mo(NC_6H_3*i*-Pr_2-2,6)$_2$L^1] (119.03(10) º). [6c]

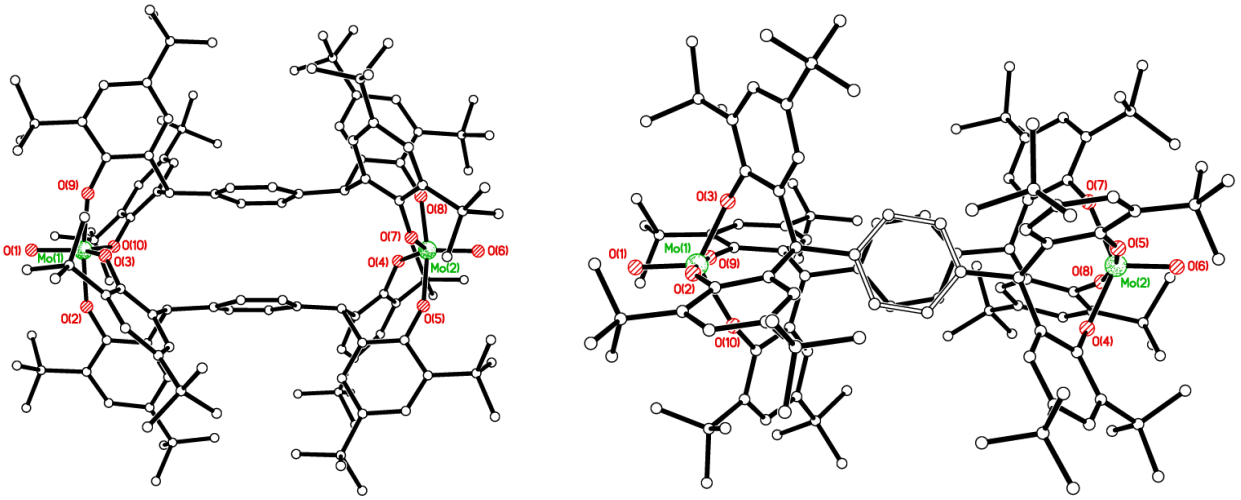

Figure 5. Two views of the molecular structure of **4**. Selected bond lengths (Å) and angles (º): Mo(1)–O(1) 1.669(4), Mo(1)–O(2) 1.886(4), Mo(1)–O(3) 1.924(4), Mo(1)–O(9) 1.867(4), Mo(1)–O(10) 1.928(4), Mo(2)–O(4) 1.942(4), Mo(2)–O(5) 1.855(4), Mo(2)–O(6) 1.672(4), Mo(2)–O(7) 1.925(4), Mo(2)–O(8) 1.878(4); O(1)–Mo(1)–O(2) 93.09(18), O(1)–Mo(1)–O(3) 118.36(18), O(2)–Mo(1)–O(9) 172.49(15), O(4)–Mo(2)–O(5) 88.45(17), O(4)–Mo(2)–O(6) 114.33(17), O(5)–Mo(2)–O(8) 169.11(15), O(6)–Mo(2)–O(7) 112.77(18), O(7)–Mo(2)–O(8) 90.46(16), Mo(1)–O(2)–C(1) 151.4(4), Mo(1)–O(3)–C(16) 136.9(4), Mo(1)–O(9)–C(101) 157.2(3), Mo(2)–O(4)–C(36) 132.7(3), Mo(2)–O(5)–C(51) 158.7(3), Mo(2)–O(8)–C(80) 156.1(3).

In the case of tungsten, use of [W(O)(O*t*-Bu)$_4$] [17] allowed facile access to the analogous 26-membered tungsten metallocycle **5**. Single crystals were obtained from a saturated acetonitrile solution at 0 ºC and are isostructural with **4**. A view of the molecular structure of **5** is shown in Figure 6, together with a space filling diagram (an alternative space filling diagram is given in the ESI, Fig. S5). As for **4**, each metal adopts a distorted trigonal bipyramidal geometry with the oxo group in the equatorial plane and pointing outwards. The cavity size is very similar to that of **4** with a W(1)···W(2) separation of 11.446 Å and a C_6H_4 ring separation of *ca*. 3.7 Å.

Two 8-membered metallocycles are formed at each end of the complex by the tetra-phenolates, with each adopting the boat conformation (as for **4**). The bite angles of the chelates are in the range 89.13(17) – 90.16(18)º, which is similar to that found (88.61(6) and 88.85(6)º) in the mononuclear tungsten complex **2**·2MeCN.

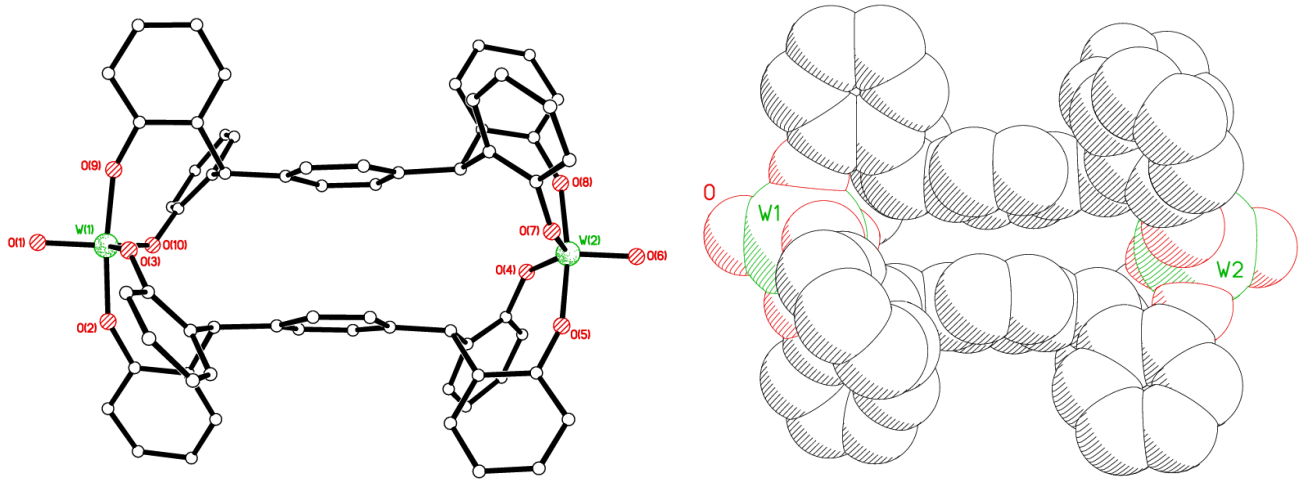

Figure 6. Left: View of the molecular structure of **5** (*tert*-butyl groups removed for clarity). Selected bond lengths (Å) and angles (º): W(1)–O(1) 1.705(4), W(1)–O(2) 1.888(4), W(1)–O(3) 1.918(4), W(1)–O(9) 1.891(4), W(1)–O(10) 1.932(4), W(2)–O(4) 1.934(4), W(2)–O(5) 1.869(4), W(2)–O(6) 1.710(4), W(2)–O(7) 1.922(4), W(2)–O(8) 1.866(4); O(1)–W(1)–O(2) 93.43(18), O(1)–W(1)–O(3) 116.58(19), O(2)–W(1)–O(9) 172.84(16), O(4)–W(2)–O(5) 89.13(17), O(4)–W(2)–O(6) 113.08(18), O(5)–W(2)–O(8) 169.51(16), O(6)–W(2)–O(7) 111.45(18), O(7)–W(2)–O(8) 90.16(18), W(1)–O(2)–C(1) 151.9(4), W(1)–O(3)–C(16) 138.0(4), W(1)–O(9)–C(101) 155.4(4), W(2)–O(4)–C(36) 134.1(3),W(2)–O(5)–C(51) 158.0(4), W(2)–O(8)–C(80) 156.1(4). Right: Space filling diagram (*tert*-butyl groups removed for clarity).

Calix[4]arenes: For comparison, the related p-*tert*-butylcalix[4]areneH$_4$ (L^3H_4) derived complexes, namely [M(O)L^3(NCMe)] (M = Mo (**6**), W (**7**)] were also prepared and structurally characterized.

In the case of molybdenum, our entry point was again [Mo(O)(O*i*-Pr)$_4$]. Following reaction with L^3H_4 in THF and subsequent work-up (MeCN), the orange/red crystalline complex [Mo(O)L^3(NCMe)] (**6**) was isolated in good yield. In the IR spectrum, there was a strong *ν*Mo=O stretch at 964 cm^{-1}. Single crystals suitable for an X-ray determination were grown from a saturated acetonitrile solution, and the molecular structure of **6** is shown in Figure 7, with selected bond lengths and angles given in the caption. The structure was twinned via a 2-fold rotation about *c* with twin law (0 –1 0, –1 0 0, 0 0 –1) with major component 90.57(2) %. One quarter of the molecule is unique. A 4-folds axis aligns along O(2)–Mo(1)–N(1)–C(12). The geometry at molybdenum is distorted octahedral, with Mo(1) positioned 0.3261 Å above

the calixarene O_4 plane. The Mo=O distance [1.685(6) Å] and Mo–O distances [1.920(3) Å] are typical. The distance across the upper rim, i.e. C(4)···C(4A) is 8.400 Å. There is no solvent of crystallisation. The methyl group of the MeCN ligand in the cavity was modelled as disordered over four, equally occupied, positions, giving an angle slightly off-linear at C(12), which is commonly seen for MeCN groups.

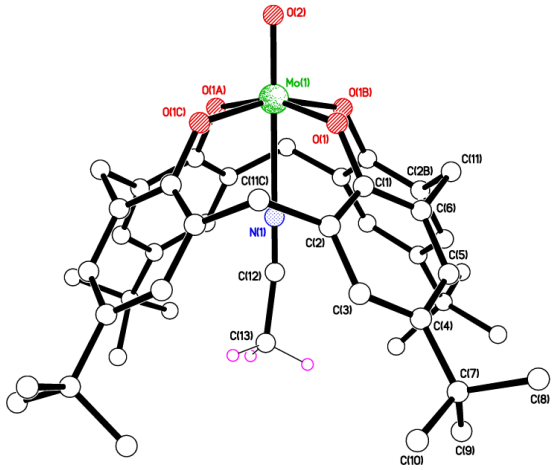

Figure 7. View of the molecular structure of **6**. Selected bond lengths (Å) and angles (°): Mo(1)–O(1) 1.920(3), Mo(1)–O(2) 1.685(6), Mo(1)–N(1) 2.424(8); O(1)–Mo(1)–O(1A) 160.44(17) O(2)–Mo(1)–N(1) 180.0.

The structure of **6** is layered with 2D sheets in the *a*/*b* plane (see Figure 8). Within layers, molecules are alternately up-down-up-down. This motif, in space group *P*4/*n*, is commonly observed for *t*Bucalix[4]areneH_4 with small, short, encapsulated guest molecules that do not protrude too far outside the calixarene cavity. [18] The motif is still adopted here, seemingly unaffected by the addition of the M=O group which fits comfortably within a cleft between the molecules.

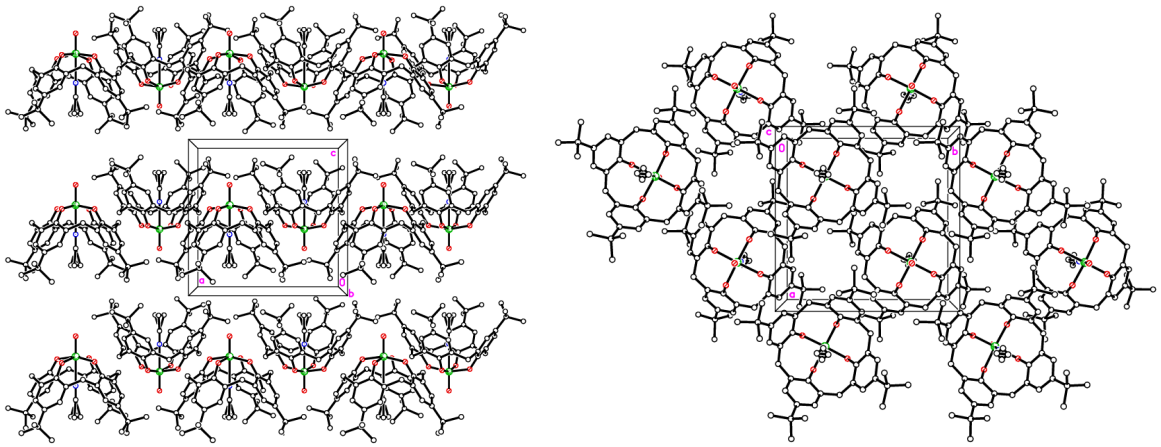

Figure 8. Views of the packing of **6**.

For tungsten, use of $[W(O)Cl_4]$ with L^3H_4 in benzene at ambient temperature led, following work-up (extraction into acetonitrile), to the isolation of $[W(Cl)_2L^3]\cdot 3.5MeCN$ (**7**·3.5MeCN). The molecular structure of **7**·3.5MeCN is shown in Figure 9, with bond lengths and angles given in the caption. The tungsten centre is, as expected, distorted octahedral with *cis*-chlorides. The calix[4]arene adopts a 'down-down-down-out' conformation, and there is one disordered MeCN in the calix cavity with the methyl group end embedded. The other MeCNs lie *exo* to the calix and reside between the tungstocalix[4]arenes. The structure of the analogous molybdenum complex $[MoCl_2L^3]$ was reported by Radius as the *tris*-benzene solvate. [20]

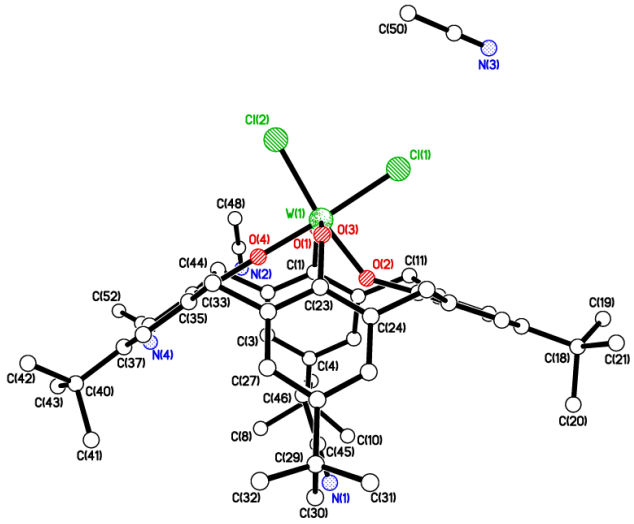

Figure 9. View of the molecular structure of **7**·3.5MeCN. Selected bond lengths (Å) and angles (°): W(1)–Cl(1) 2.3431(7), W(1)–Cl(2) 2.3308(7), W(1)–O(1) 1.8979(19), W(1)–O(2) 1.8892(19), W(1)–O(3) 1.8975(18), W(1)–O(4) 1.8447(19); Cl(1)–W(1)–Cl(2) 85.86(3), Cl(1)–W(1)–O(2) 85.44(6), W(1)–O(1)–C(1) 127.03(16), W(1)–O(2)–C(12) 143.91(17), W(1)–O(3)–C(23) 126.35(15), W(1)–O(4)–C(34) 179.02(19).

The tungsten oxo calix[4]arene was prepared via a modification of the method reported by Floriani *et al*, [11] namely reaction of $[W(O)Cl_4]$ with L^3H_4 in refluxing toluene. Subsequent crystallisation from acetonitrile afforded $[W(O)L^3(NCMe)]$ (**8**) which is isostructural with **6**. A view of **8** is shown in Figure 10, with selected bond lengths and angles given in the caption. A quarter of the molecule is the asymmetric unit as it lies on a 4-fold axis, with W(1), O(2), N(1) and C(12) lying exactly on the axis. The

data were merohedrally 2-fold twinned via twin law 1 0 0, 0 –1 0, 0 0 –1. The complex is mononuclear with O=W-NCMe along the 4-fold axis. There is no solvent of crystallisation. As for **6**, the methyl group of the MeCN was modelled as disordered over four equally occupied sets of positions (determined by the 4-fold axis). Although examples of coordinated MeCN molecules in calix[4]arene cavities are well known, few are bent. Indeed, analysis of twenty one such transition metal bound acetonitriles, [21] found only one to have the N-C-Me angle more than 10° away from linear (169.67°). [21e]

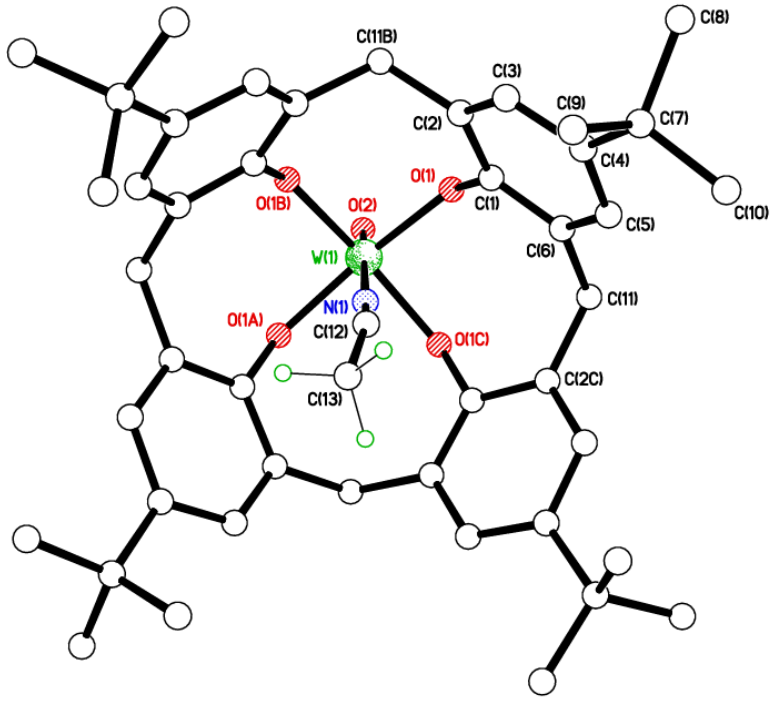

Figure 10. View of the molecular structure of **8**. Selected bond lengths (Å) and angles (°): W(1)–O(1) 1.913(2), W(1)–O(2) 1.702(4), W(1)–N(1) 2.412(5); O(1)–W(1)–O(2) 99.87(7), W(1)–O(1)–C(1) 132.93(19), N(1)–C(12)-C(13) 163.2(17).

In the packing of **8**, there are layers in the *a/b* plane with molecules alternately anti-parallel (see Figure 11). As with **6**, which is isomorphous, the packing motif is similar to several *t*-Bucalix[4]areneH_4 solvates. [18]

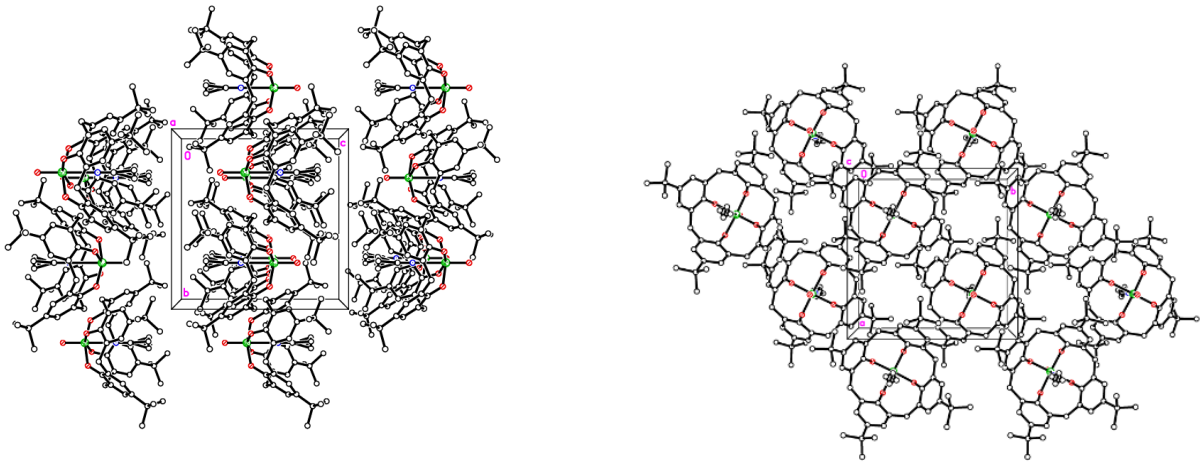

Figure 11. Views of the packing in **8**.

Surprisingly, reaction of [W(O)(O*t*-Bu)$_4$] and L^3H_4 in refluxing toluene afforded after work-up, orange/red prisms of the bis(*tert*-butoxide) complex [W(O*t*-Bu)$_2L^3$]·MeCN (**9**·MeCN) in good yield. Single crystals suitable for X-ray diffraction were grown from a saturated acetonitrile solution at ambient temperature. The molecular structure of [W(O*t*-Bu)$_2L^3$]·MeCN (**9**·MeCN) is shown in Figure 12. The metal adopts an octahedral geometry with the *tert*-butoxide groups occupying *cis* positions [O(5)–W(1)–O(6) = 89.51(9)°]. The calix[4]arene adopts a down-down-down-out conformation. One molecule of MeCN per W complex resides inside the calixarene cavity (not metal bound) with the methyl group deepest inside and the nitrogen pointing outwards. Prolonged reflux (>48 h) of **9** in MeCN led to the isolation of a yellow complex which was identified by single crystal X-ray diffraction to be the oxo complex **8**.

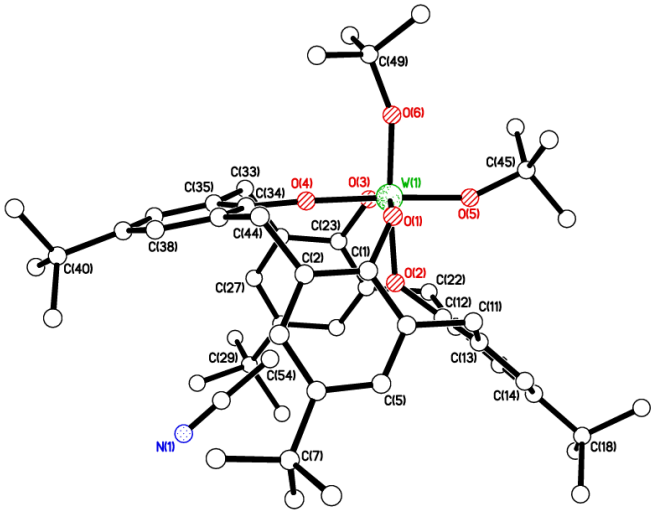

Figure 12. View of the molecular structure of **9**. Selected bond lengths (Å) and angles (°): W(1)–O(1) 1.9548(19), W(1)–O(2) 1.9440(19), W(1)–O(3) 1.9532(19), W(1)–O(4) 1.8789(19), W(1)–O(5) 1.841(2), W(1)–O(6) 1.849(2); O(1)–W(1)–O(3) 162.45(8), O(2)–W(1)–O(4) 92.42(8), W(1)–O(1)–C(1) 123.11(17), W(1)–O(2)–C(12) 131.00(17), W(1)–O(3)–C(23) 124.38(16), W(1)–O(4)–C(34) 176.96(18), W(1)–O(5)–C(45) 154.12(19), W(1)–O(6)–C(49) 157.3(2).

Ring opening polymerisation studies

General: The ability of these complexes to act as catalysts for the ring opening polymerization (ROP) of ε-caprolactone (ε-CL) (Table 1 and Table S1, ESI) and δ-valerolactone (δ-VL) / ω-pentadecalactone (ω-PDL) (Table 2 and table 2, ESI) has been investigated. The non-calix[4]arene complexes **1**, **2** and **4**, **5**, for which the metal geometry is best described as distorted trigonal bipyramidal, afforded the highest yields of polymer, and given this, our investigations here have focussed primarily on these four complexes. The metallocalix[4]arenes **6** – **9**, where the metal is distorted octahedral, are not as active, and the products obtained may be better described as oligomers. [22]

ε-caprolactone (ε-CL)

From the tables below and the kinetic data in the ESI, it can be seen that the molybdenum compounds **1** and **4** out-performed their tungsten analogues **2** and **5**. The systems do not exhibit good control, for example in the case of the Mo-based systems **1** and **4**, the polydispersity values are wide (M_w/M_n = 1.29 to 3.29). However, the relationship between the monomer mole ratio and the number average molecular weight values is near linear (e.g. for **4** see runs 35 to 38 –Table S1, ESI), indicating that this is a living polymerization process. For **1**, only trace PCL was observable for temperatures below 50 °C, however on increasing the temperature from 50 to 130 °C using 500:1 (ε-CL:catalyst) (runs 18 - 24, Table S1, ESI), the ability to form PCL dramatically increased with greater than 98 % conversion possible over 1 h at 130 °C. From a kinetic study (Fig. S10, ESI), it was observed that the polymerization rate exhibited near first order dependence on the CL concentration at 130 °C. Using [CL]:[Mo] = 500:1, the observed molecular weights were lower than the calculated values, suggesting the presence of transesterification processes. Furthermore, the MALDI-TOF spectra of the PCL revealed peaks separated by 114 mass units, and there was evidence of second and third populations. For example, in the case of **1** (run 21, table S1, Figs. S11

and S12, ESI), peaks of the spectrum can be assigned to 2876 (cyclic PCL), 2894 (acid, monosodium) and 2915 (disodium) for $H[O(CH_2)_2CO]_nOH$ (n= 20), and 2989 (cyclic), 3007 (acid, monosodium), 2029 (acid, disodium) (n = 26) etc….

Table 1. ROP of ε-CL using complex **1 - 9**

Run	Cat.	CL:M	T/℃	t/h	Conv.%[a]	*Mn*[b]	Mn_{Calcd}[c]	PDI[d]
1	**1**	250:1	130	24	99.1	24430	28190	2.26
2	**2**	250:1	130	24	98.6	5820	28140	1.32
3	**3**	250:1	130	48	97.5	38000	27820	1.85
4	**4**	250:1	130	48	99.6	29650	28420	1.91
5	**5**	250:1	130	24	94.6	21240	26990	1.76
6	**6**	250:1	130	24	99.1	5230	28280	1.12
7	**7**	250:1	130	48	99.3	3600	28340	1.61
8	**8**	250:1	130	48	94.5	4980	22970	1.10
9	**9**	250:1	130	24	39.0	5260	11130	1.10

[a] Determined by ^{1}H NMR spectroscopy. [b] M_n from GPC in THF and were corrected with a Mark-Houwink factor of 0.56. [c] Calculated from ($[Monomer]_o/[M]_o$) x conv. (%) x Monomer molecular weight. [d] From GPC. [e] low yield.

In the case of **4**, at ambient temperature (14 ºC) the system was inactive, although at 25 ºC 67% conversion was observed over 24 h albeit in low yield. Increasing the temperature to 60 ºC and above resulted in conversions > 90%, and at 130 ºC using a ratio of 500:1, conversions in excess of 99% were achievable over 1 h. As for **1**, the kinetics revealed a near first order dependence on the ε-CL concentration (Fig. S12, ESI). There is again evidence for the presence of transesterification processes, with observed molecular weights being lower than the calculated values, and as well as the main family of peaks, minor second and third populations observed in the MALDI-TOF spectrum (see Fig. S14, ESI). Similar assignments as for **1** can be attributed to the MALDI-ToF spectrum of PCL using **4** (run 32, Table S1), for example 2191 (cyclic), 2209 (acid, monosodium) and 2232 (disodium). On comparing results for **1** *versus* **4**, the % conversions are comparable over most temperatures and the kinetic parameters are similar, with only a small benefit observed from the presence of the second metal in **4** (note in Tables 1

and S1, [M] takes into account the number of metals present, *i.e.* for **4** this would involve using half the concentration compared with **1**). Interestingly, the observed M_n values for **4** tend to be somewhat lower (less than half) than those observed for **1**.

δ-valerolactone (δ-VL)

Complexes **1** - **9** were also evaluated as catalysts for the ROP of δ-VL (see Table 2 and Table S2, ESI). Using compound **1**, the conditions of time, temperature and [M]:[δ-VL] were varied (see runs 1-15, Table S2). Best observed results were achieved at 130 ºC using [M]:[δ-VL] at 1:500 over 24 h. As in the case of the ROP of ε-CL, the molybdenum complexes **1** and **4** outperformed their tungsten counter-parts **2** and **5** (see kinetic plots Figs. S16 and S17). Results for **5** were very poor, and this was attributed to the limited solubility of **5** in toluene. As for the ROP of ε-Cl, there was evidence of significant transesterification and nearly all observed M_n values were significantly lower than the calculated values. The MALDI-TOF spectra could be interpreted using the formula $H[O(CH_2)_4CO]_nOH$, for example in the case of **2** at 110 ºC (see Fig. S18, ESI).

Table 2. ROP of δ-VL using complexes **1 - 9**

Run	Cat.	VL:M	T/℃	t/h	Conv.%[a]	*Mn*[b]	Mn_{Calcd}[c]	PDI[d]
1	**1**	500:1	130	24	99.1	31000	49610	2.03
2	**2**	500:1	130	24	86.6	3500	43350	1.10
3	**3**	500:1	130	24	95.3	8020	47710	1.71
4	**4**	125:1	130	24	99.4	12880	12440	2.20
5	**5**	125:1	130	24	87.7	10380	10980	1.41
6	**6**	250:1	130	24	82.0	5240	20520	1.11
7	**7**	250:1	130	24	82.9	4870	20750	1.73
8	**8**	250:1	130	24	97.5	4630	24400	1.56
9	**9**	250:1	130	24	46.0	3210	11510	1.15

[a] Determined by ^{1}H NMR spectroscopy. [b] M_n from GPC in THF and were corrected with a Mark-Houwink factor of 0.57. [c] Calculated from $([Monomer]_o/[M]_o)$ x conv. (%) x Monomer molecular weight. [d] From GPC.

ROP of ω-pentadecalactone (ω-PDL): In order to enhance the thermal properties of the polymers obtained herein, we also investigated the ROP of the macrolactone ω-pentadecalactone (ω-PDL). Unfortunately, none of the systems herein proved to be effective as catalysts for the ROP of ω-PDL either in solution at high temperatures (140 ºC) or as melts. Bouyahyi and Duchateau noted that it is more difficult to achieve the ROP of ω-PDL *versus* ε-CL. [23]

In conclusion, we have isolated and structurally characterized a number of oxo species of molybdenum and tungsten, all of which are bound by chelating aryloxide ligands. Use of the di-phenol 2,2′-ethylidenebis(4,6-di-*tert*-butylphenol) L^1H_2 leads, in the absence of alkali metal incorporation, to monomeric $MO(L^1)_2$ type complexes, whilst the tetraphenol α,α,α′,α′-tetrakis(3,5-di-*tert*-butyl-2-hydroxyphenyl)-*p*-xyleneH_4 (L^2H_4) affords 26-membered metallocycles of the form $\{[Mo(O)]L^2\}_2$. The unexpected formation of the complex $[W(O\textit{t}\text{-Bu})_2L^3]$ from p-*tert*-butylcalix[4]areneH_4 (L^3H_4) and $[W(O)(O\textit{t}\text{-Bu})_4]$ is also reported. Screening of these complexes for the ROP of the cyclic esters ε-caprolactone (ε-CL) and δ-valerolactone (δ-VL) revealed that the molybdenum complexes tend to perform best, particularly those derived from L^1 and L^2, where the metal is 5-coordinate (distorted trigonal bipyramidal), although with poor control. There was little sign of any significant beneficial cooperative effect resulting from the presence of the second metal centre in the macrocyclic complexes **4** and **5**. The metallocalix[4]arene systems (**6 - 9**), in which the metal is 6-ccordinate (distorted octahedral), were less active. None of the systems screened were capable of the ROP of the macrolactone ω-pentadecalactone (ω-PDL) either in solution or as melts.

Experimental

General: All manipulations were carried out under an atmosphere of dry nitrogen using conventional Schlenk and cannula techniques or in a conventional nitrogen-filled glove box. Hexane and toluene were refluxed over sodium. Acetonitrile was refluxed over calcium hydride. THF, DME, and diethylether were dried over sodium benzophenone. All solvents were distilled and degassed prior to use. IR spectra (nujol

mulls, KBr windows) were recorded on a Nicolet Avatar 360 FT IR spectrometer; ^{1}H NMR spectra were recorded at room temperature on a Varian VXR 400 S spectrometer at 400 MHz or a Gemini 300 NMR spectrometer or a Bruker Advance DPX-300 spectrometer at 300 MHz. The ^{1}H NMR spectra were calibrated against the residual protio impurity of the deuterated solvent. Elemental analyses were performed by the elemental analysis service at the London Metropolitan University, the Department of Chemistry, the University of Hull and at the Shanghai Institute of Organic Chemistry (SIOC), Chinese Academy of Sciences. The precursors [Mo(O)(O*i*-Pr)$_4$] and [W(O)(O*t*-Bu)$_4$] were prepared by the literature methods. [17, 19] The pro-ligands L^2H_4 and L^3H_4 were prepared as described previously. [24] All other chemicals were purchased from Sigma Aldrich.

Synthesis of [Mo(O)(L^1)$_2$]·hexane (**1**·hexane)

L^1H_2 (2.21 g, 5.04 mmol) was dried at 80 °C for 12 h under vacuum. On cooling, diethylether (30 mL) was added and the system was cooled to –78 °C, following which *n*-butyllithium (6.30 mL, 1.6 M, 10.08 mmol) was added. The system was allowed to warm to ambient temperature and left to stir for 12 h. The system was again cooled to –78 °C and solid [Mo(O)Cl$_4$] (0.64 g, 2.52 mmol) was added. After stirring for 12 h, volatiles were removed *in vacuo* and the residue was extracted into hexane (30 mL). Cooling to 0°C afforded **1**·hexane as blue crystals. Yield 1.54g, 57%. Found C 73.39, H 10.17 %. $C_{66}H_{100}MoO_5$ requires C 73.98, H 9.60%. M.S. 986 $(M^+ + H - \text{hexane})^+$, 438 $(MH^+ - L^1 - MoO)$. IR: 1762w, 1593s, 1293w, 1268m, 1225s, 1160s, 1114m, 1070w, 1024w, 963s, 924m, 873s, 844s, 757m, 567s. ^{1}H NMR (C_6D_6, sample dried *in-vacuo* for 12 h) δ: 7.39 (m, 8H, aryl*H*), 4.42 (q, J_{HH} 4.0 Hz, 2H, C*H*), 1.62 (d, J_{HH} 4.0 Hz, 6H, CH*Me*), 1.42 (s, 36H, C(CH_3)$_3$), 1.29 (s, 36H, C(CH_3)$_3$).

Synthesis of [W(O)(L^1)$_2$]·2MeCN (**2**·2MeCN)

[W(O)(O*t*-Bu)$_4$] (0.50 g, 1.02 mmol) and L^1H_2 (0.90 g, 2.05 mmol) were stirred in Et_2O (30 mL) for 30 min., and then the volatiles were removed *in-vacuo*. Another batch of Et_2O (30 mL) was added and the cycle was repeated 4 times. Subsequent extraction of the residue into MeCN (30 mL) afforded 0.69g of red prisms of **2**;

cooling of the mother liquor afforded further crops of crystals, overall yield 0.99g, 91%. Found C 66.31, H 8.65, N 0.97%. $C_{62}H_{91}WNO_5$ (sample dried *in vacuo* for 2 h, – MeCN) requires C 66.83, H 8.23, N 1.26%. M.S. 1115 $(M^+ + H - MeCN)^+$, 675 $(M^+ + H - MeCN - L^2H_2)^+$. IR: 1302w, 1237s, 1162s, 1014m, 966s, 852s, 796w, 757w, 726m, 564m, 487w, 414w. ^{1}H NMR (C_6D_6) δ: 7.35, 7.27, 7.16 (3x m, 8H, aryl*H*), 3.93 (q, J_{HH} 4.0 Hz, 2H, C*H*), 1.83 (d, J_{HH} 4.0 Hz, 6H, CH*Me*), 1.61 (s, 36H, C(CH_3)$_3$), 1.26 (s, 36H, C(CH_3)$_3$). ^{13}C NMR (C_6D_6) δ: 159.70, 143.82, 138.02, 134.87, 121.56, 119.72, 86.14, 38.32, 35.40, 34.66, 31.83, 30.60, 19.15.

Synthesis of {Mo(O)(L^1)(μ-O)Li(THF)(MeCN)}$_2$·2MeCN (**3**·2MeCN)

LiO*t*-Bu (15.8 mL, 1.0 M in THF, 15.8 mmol) was added to [Mo(O)Cl_4] (1.00 g, 3.94 mmol) in diethylether (30 mL) at –78 °C, and the system was allowed to warm to room temperature whilst being stirred. Pre-dried L^1H_2 (1.73 g, 3.94 mmol) in diethylether (20 mL) was then added. After stirring for 1 h, the volatiles were removed *in vacuo*, and the residue was extracted into MeCN (30 mL). On prolonged standing (2 – 3 days) at 0 °C, large orange/brown prisms of **3** were formed. Yield: 1.17 g, 41%. Further crops were obtained by concentration and cooling of the mother liquor. Overall isolated yield 1.83g, 64%. Found C 63.42, H 7.87, N 3.88%. $C_{76}H_{116}N_4Li_2Mo_2O_{10}$ requires C 62.88, H 8.06, N 3.86%. M.S. 1452 (MH^+), 1209 (MH^+ – 4MeCN – THF – Li), 1121 (MH^+ – 4MeCN – 2THF – Li – O), 1114 (MH^+ – 4MeCN – 2THF – 2Li – O). IR: 2301w, 2270w, 2251w, 1414w, 1366m, 1326w, 1299m, 1272m, 1236m, 1201w, 1164m, 1141w, 1117w, 1042m, 973s, 932w, 918w, 901w, 880w, 873w, 852w, 836w, 800w, 782w, 771w, 756w, 733m, 559w, 533w, 459w, 434w.

Synthesis of {[Mo(O)]L^2}$_2$ (**4**)

L^2H_2 (0.47 g, 0.51 mmol) was dried at 80 °C for 12 h under vacuum. On cooling, diethylether (30 mL) was added and the system followed by [Mo(O)(O*i*-Pr)$_4$] (0.18 g, 0.52 mmol) in diethylether (30 mL). After stirring for 2 h, volatiles were removed *in vacuo*, and the cycle was repeated two more times. The residue was extracted into hexane (30 mL) and on prolonged standing at 0 °C afforded **4**. Yield 0.29g, 56%. Found C

76.07, H 10.24%. $C_{128}H_{172}Mo_2O_{10}$·5hexane requires C 76.10, H 9.78%. M.S. (positive nanoelectrospray): 1950 (M^+ – MoO). IR: 1606w, 1504m, 1407m, 1364s, 1331m, 1280m, 1259s, 1249s, 1202m, 1190m 1177m, 1152m, 1123m, 1084s, 1051w, 1021m, 960s, 917w, 886m, 859m, 808s, 776w, 723s. ^{1}H NMR (C_6D_6) δ: 7.69 (s, 3H, aryl*H*), 7.32 (s, 4H, aryl*H*), 7.28 (m, 4H, aryl*H*), 7.10 (m, 13H, aryl*H*), 4.18 (m, 2H, C*H*), 1.58 (s, 36H, C(CH_3)$_3$), 1.08 (s, 36H, C(CH_3)$_3$).

Synthesis of {[W(O)]L^2}$_2$ (**5**)

L^2H_2 (0.47 g, 0.51 mmol) was dried at 80 °C for 12 h under vacuum, then on cooling [W(O)(O*t*-Bu)$_4$] (0.50 g, 1.02 mmol) in toluene (30 mL) was added and the system was heated for 1h, following which the volatiles were removed *in vacuo*. The cycle was repeated 3 times. The residue was extracted into MeCN (30 mL) and on prolonged standing at 0 °C orange/red prisms of **5** formed. Yield 0.41g, 36%. Found C 70.87, H 7.79%. $C_{128}H_{172}W_2O_{10}$·2.5toluene requires C 70.78, H 7.84%. M.S. (solvent-free MALDI): 2238 (M^+). IR: 1285w, 1260s, 1197w, 1093s, 1025s, 880w, 864w, 804s, 723w, 564w, 476w, 415m. ^{1}H NMR ($CDCl_3$) δ: 7,46 (m, 5H, aryl*H*), 7.20 (m, 2H, aryl*H*), 7.13 (m, 3H, aryl*H*), 6.98 (overlapping m, 6H, aryl*H*), 6.90 (m, 3H, aryl*H*), 6.84 (m, 2H, aryl*H*), 6.59 (m, 3H, aryl*H*), 5.55 (m, 1H, C*H*), 5.11 (m, 1H, C*H*), 4.66 (m, 1H, C*H*), 4.58 (m, 1H, C*H*), 1.33 (s, 18H, C(CH_3)$_3$), 1.32 (s, 9H, C(CH_3)$_3$), 1.23 (s, 9H, C(CH_3)$_3$), 1.22 (s, 9H, C(CH_3)$_3$), 1.10 (s, 9H, C(CH_3)$_3$), 1.08 (s, 9H, C(CH_3)$_3$), 1.06 (s, 9H, C(CH_3)$_3$).

Synthesis of [Mo(O)L^3(NCMe)] (**6**)

To pre-dried L^3H_4 (3.26 g, 5.02 mmol) in toluene (30 mL) was added [Mo(O)(O*i*-Pr)$_4$] (1.75 g, 5.02 mmol) and the system was refluxed for 12 h. Following removal of volatiles, the residue was extracted into MeCN (30 mL), and on prolonged standing at 0 °C red/brown prisms of **6** formed. Yield 0.59g, 15%. Found C 69.36, H 6.98, N 1.79 %. $C_{46}H_{55}NMoO_5$ requires C 69.24, H 6.95, N 1.76 %. M.S. (APCI; ASAP): 797 (M^+), 757 (M^+ – MeCN). IR: 2311w, 2284w, 1750w, 1646w, 1601w, 1308m, 1286m, 1239m, 1192s, 1123w, 1104m, 1029m, 964s, 936w, 916m, 889w, 871s, 797s, 763w, 739m, 722m, 678w, 632w, 558s, 504m, 428s. The sample proved to be too insoluble to obtain useful ^{1}H NMR data.

Synthesis of [$W(Cl)_2L^3$]·3.5MeCN (**7**·3.5MeCN)

[WCl_6] (1.16 g, 2.93 mmol) and pre-dried L^3H_4 (1.90 g, 2.93 mmol) were stirred in CH_2Cl_2 (30 mL) for 12 h. Following removal of volatiles, the purple residue was extracted into MeCN (20 mL) and left to stand at room temperature to afford **7** as purple prisms, Yield: 1.31g, 42.8%. Found C 58.20, H 6.46%. $C_{44}H_{52}WCl_2O_4$ (sample dried *in-vacuo* for 12h) requires C 58.74, H 5.83%. M.S. (positive nanoelectrospray): 900 (M^+ – 3.5MeCN), 864 (M^+ – 3.5MeCN – Cl), 829 (M^+ – 3.5MeCN – 2Cl). IR: 2260w, 2245w, 1414w, 1365s, 1309m, 1287m, 1261m, 1240m, 1192s, 1105m, 1020w, 981m, 939w, 917m, 889w, 872m, 839s, 798s, 765w, 722m, 679w. ^{1}H NMR ($CDCl_3$) δ: 7.26 – 7.05 (3x m, 8H, aryl*H*), 4.65 (d, J_{HH} 12.50 Hz, 4H, *endo*-CH_2), 3.31 (d, J_{HH} 12.50 Hz, 4H, *exo*-CH_2), 2.01 (bs, 6H, 2*Me*CN), 1.18 (s, 36H, C(CH_3)$_3$), –0.17 (bs, 3H, *Me*CN).

Synthesis of [$W(O)L^3$(NCMe)] (**8**)

[$W(O)Cl_4$] (1.00 g, 2.93 mmol) and pre-dried L^3H_4 (1.90 g, 2.93 mmol) were refluxed in benzene (30 mL) for 12 h. Following removal of volatiles, the orange/brown residue was extracted into toluene (20 mL), which was then removed *in-vacuo*, and the residue extracted into MeCN (20 mL). Prolonged standing (over 2 - 3 days) at room temperature afforded crystalline **8** in a yield 44% (1.13g). Found C 62.64, H 6.32, N 1.78 %. $C_{46}H_{55}NWO_5$ requires C 62.37, H 6.26, N 1.58%. M.S. (nano-ESI, negative): 873 (MH^+ – NCMe). IR: 2316w, 2280w, 1603w, 1569w, 1365ms, 1306m, 1286m, 1271m, 1261w, 1239w, 1192m, 1121w, 1103m, 1030w, 978m, 916w, 872m, 838m, 816m, 797w, 762w, 722m, 696w, 677w, 559m, 531w, 503w, 465w, 422w. ^{1}H NMR (CD_2Cl_2) δ: 7.34 (m, 4H, aryl*H*), 7.15 (m, 5.4H, aryl*H*)*, 4.71 (d, 4H, J_{HH} 14.0 Hz, *endo*-CH_2), 4.56 (d, 0.66H, J_{HH} 12.4 Hz, *endo*-CH_2)*, 3.53 (d, 4H, J_{HH} 14.0 Hz, *exo*-CH_2), 3.31 (d, 0.66H, J_{HH} 12.4 Hz, *exo*-CH_2)*, 2.32 (s, 0.25H, CH_3 of toluene), 1.95 (s, 3H, *Me*CN), 1.34 (m, 18H, C(CH_3)$_3$), 1.18 (m, 21H, C(CH_3)$_3$)*. *The ^{1}H NMR indicates there is a second species present (~ 8%) which is consistent with the presence of the toluene solvate reported by Floriani. [10]

Synthesis of [W(O*t*-Bu)$_2$L^3]·MeCN (**9**·MeCN)

[W(O)(O*t*-Bu)$_4$] (0.50 g, 1.02 mmol) and pre-dried L^{3}H$_4$ (0.66 g, 1.02 mmol) were stirred in diethylether (30 mL) for 1h, following which the volatiles were removed *in vacuo*. The cycle was repeated 3 times. The residue was extracted into MeCN (30 mL) and on prolonged standing (2 – 3 days) at ambient temperature orange/red prisms of **9** formed. Yield: 0.92g, 88%. Found C 63.96, H 7.42, N 1.47% (should be no space) . $C_{54}H_{73}NWO_6$ requires C 63.83, H 7.24, N 1.38%. M.S. (solvent-free MALDI): 1016 (M^+), 974.5 (M^+ – MeCN), 844. 5 (M^+ – MeCN – *t*Bu – *t*BuO), 828 (M^+ – MeCN – 2*t*BuO). IR: 1747w, 1260s, 1204w, 1158w, 1095bs, 1017s, 962w, 943w, 933w, 799s, 722s, 686w. ^{1}H NMR (C_6D_6) δ: 7.27 (bs, 4H, aryl*H*), 7.13 (bs, 4H, aryl*H*), 4.83 (d, 4H, *J* 14.0 Hz, *endo*-CH_2), 3.53 (d, 4H, *J* 14.0 Hz, *exo*-CH_2), 1.28 (s, 18H, *t*BuO), 1.26 (s, 18H, *t*Bu), 0.88 (s, 18H, *t*Bu), 0.35 (s, 3H, *Me*CN). ^{13}C NMR (C_6D_6) δ: 162.33, 160.40, 145.69, 145.23, 133.84, 130.44, 127.51, 125.66, 123.54, 115.83, 87.21, 35.65, 34.11, 33.33, 31.77, 31.22, 30.22, –0.49. Prolonged reflux (48 h) of **9** in MeCN led to the isolation of **8**.

Ring open polymerization (ROP) procedures

ε-Caprolactone: Typical polymerization procedures are as follows. A toluene solution of **9** (0.010 mmol, in 1.0 mL toluene) was added into a Schlenk tube in the glove-box at room temperature. The solution was stirred for 2 min, and then ε-caprolactone (2.5 mmol) along with 1.5 mL toluene was added to the solution. The reaction mixture was then placed into an oil bath pre-heated to the required temperature, and the solution was stirred for the prescribed time. The polymerization mixture was then quenched by addition of an excess of glacial acetic acid (0.2 mL) into the solution, and the resultant solution was then poured into methanol (200 mL). The resultant polymer was then collected on filter paper and was dried *in vacuo*.

Kinetic studies

The polymerizations were carried out at 130 °C in toluene (2 mL) using 0.010 mmol (for **1** and **2**) and 0.005 mmol (for **4** and **5**) of complex. The molar ratio of monomer to initiator was fixed at 500:1, and at appropriate time intervals, 0.5 μL aliquots were removed (under N_2) and were quenched with wet $CDCl_3$. The percent conversion of monomer to polymer was determined by ^1H NMR spectroscopy.

Crystal Structure Determinations

The diffraction data was collected on a variety of modern diffractometers equipped with CCD, hybrid pixel array, or image plate detectors. X-ray sources were either conventional or micro-focus sealed tubes or rotating anodes generating either Mo-Kα or Cu-Kα X-radiation. Full details are presented in Table 3 and in the deposited cif files. Structures were solved and refined routinely [25] except as follows: in **1**·hexane the hexane of crystallisation is disordered across a symmetry element so H atoms were not modelled for this molecule and two of the unique C atoms were modelled as 2-fold disordered each at 50% occupancy; for **2**·2MeCN both MeCN molecules were modelled as fully 2-fold disordered with those at N(1) and N(2) having major site occupancy of 61.2(8)% and 71.5(11)% respectively; for **3**·2MeCN one ^{t}Bu group at C(23) was modelled with the methyl groups 2-fold disordered with major component occupancy of 76.5(11)%; in **4** the *t*-Bu group at C(42) was similarly modelled with major site occupancy of 66(2)%; in **5** the *t*-Bu group at C(42) was modelled similarly with major component occupancy of 63.8(14)% while that at C(111) was modelled with the whole *t*-Bu group split over two sets of positions with major component occupancy of 65.1(11)%; in **6** the methyl group of the MeCN ligand was modelled as disordered over four equally occupied (25% as dictated by the 4-fold symmetry) positions. This gave an N(1)–C(12)–C(13) angle slightly off-linear at C(12) which is commonly seen for MeCN groups and best modelled the observed electron density. The diffraction data for **6** were twinned via a 2-fold rotation about *c* with twin law (0 –1 0, –1 0 0, 0 0 –1) with major twin component 90.57(2)%. For **7**·3.5MeCN one MeCN is disordered across a symmetry element, so was refined as half occupied. The C=N part of the MeCN in the calixarene cavity was modelled as disordered over two sets of positions with major component occupancy 78.5(8)% and one *t*-Bu group at C(18) was modelled with the Me groups 2-fold

disordered with major component occupancy 67.0(15)% For **8** the diffraction data were merohedrally 2-fold twinned via twin law (1 0 0, 0 –1 0 , 0 0 –1) with major twin component 63.7(2)%. Modelling this twinning reduced R_1 from 9% to <3%. The coordinated MeCN was modelled as described for **6**. For **9** the *t*-Bu group at C(40) was modelled a 2-fold disordered with major component occupancy 50.4(6)%. In all cases where disorder was modelled, anisotropic displacement and geometric parameter restraints were applied to support the refinement. CCDC 1577643 and 1861428-1861436 contain the supplementary crystallographic data for this paper. These data can be obtained free of charge from The Cambridge Crystallographic Data Centre via www.ccdc.cam.ac.uk/data_request/cif.

Table 3. Crystallographic data for **1**·hexane, **1**·2MeCN, **2**·2MeCN, **3**·2MeCN and **4**.

Compound	**1**·hexane	**1**·2MeCN	**2**·2MeCN	**3**·2MeCN	**4**
Formula	$C_{66}H_{102}MoO_5$	$C_{64}H_{94}MoN_2O_5$	$C_{64}H_{94}WN_2O_5$	$C_{76}H_{116}Li_2Mo_2N_4O_{10}$	$C_{128}H_{172}Mo_2O_{10}$
Formula weight	1071.41	1067.35	1155.26	1451.48	2062.53
Crystal system	Monoclinic	Monoclinic	Monoclinic	Orthorhombic	Triclinic
Space group	C2/c	$P2_1/c$	$P2_1/c$	$P2_12_12$	$P\bar{1}$
a (Å)	12.4077(5)	12.3081(6)	12.20640(10)	18.8177(14)	17.8943(6)
b (Å)	17.8693(8)	18.8028(10)	18.65840(10)	19.7659(15)	18.8664(6)
c (Å)	27.6221(12)	27.2978(13)	27.3246(2)	10.7727(8)	22.3021(8)
α (º)	90	90	90	90	69.326(3)
β (º)	92.320(2)	92.387(4)	91.9900(10)	90	89.921(3)
γ (º)	90	90	90	90	64.793(3)
V (Å^3)	6119.3(5)	6312.(5)	6219.48(8)	4006.9(5)	6274.1(4)
Z	4	4	4	2	2
Temperature (K)	150(2)	150(2)	100(2)	150(2)	100(2)
Wavelength (Å)	0.71073	0.71073	0.71073	0.71073	1.54184
Calculated density (g.cm^{-3})	1.163	1.123	1.234	1.203	1.092
Absorption coefficient (mm^{-1})	0.26	0.25	1.90	0.37	2.04
Transmission factors (min./max.)	0.851, 0.962	0.962, 0.966	0.777, 1.000	0.861, 0.944	0.670, 1.000
Crystal size (mm^3)	0.64 × 0.33 × 0.15	0.27 × 0.22 × 0.15	0.18 × 0.11 × 0.06	0.42 × 0.26 × 0.16	0.08 × 0.07 × 0.01
θ(max) (°)	28.9	26.9	27.5	29.7	68.3
Reflections measured	26161	29575	137895	45268	97774
Unique reflections	7274	13335	14242	11273	22790
R_{int}	0.020	0.040	0.032	0.096	0.067
Reflections with $F^2 > 2\sigma(F^2)$	6574	8155	14088	8820	17480
Number of parameters	353	677	735	464	1326
R_1 [$F^2 > 2\sigma(F^2)$]	0.033	0.034	0.025	0.051	0.085
wR_2 (all data)	0.088	0.073	0.058	0.102	0.244

GOOF, *S*	1.10	0.82	1.19	1.01	1.06
Largest difference peak and hole (e Å^{-3})	0.74 and –0.61	0.51 and –0.28	1.34 and –0.77	1.42 and –0.92	3.71 and –1.22

Table 3 con't. Crystallographic data for **5**, **6**, **7**·3.5MeCN, **8** and **9**·MeCN

Compound	**5**	**6**	**7**·3.5MeCN	**8**	**9**·MeCN
Formula	$C_{128}H_{172}W_2O_{10}$	$C_{46}H_{55}MoNO_5$	$C_{51}H_{62.5}WCl_2N_{3.5}O_4$	$C_{46}H_{55}WNO_5$	$C_{54}H_{73}WNO_6$
Formula weight	2238.35	797.85	1043.29	885.76	1015.98
Crystal system	Triclinic	Tetragonal	Monoclinic	Tetragonal	Tetragonal
Space group	*P*$\bar{1}$	*P*4/*n*	*I*2/*a*	*P*4/*n*	*I*4$_1$/*a*
a (Å)	17.9604(4)	12.7438(4)	26.8222(19)	12.76192(10)	27.38560(10)
b (Å)	18.9135(5)		10.0205(7)		
c (Å)	22.3389(5)	12.5551(8)	40.384(3)	12.52433(18)	26.8480(2)
α (º)	69.394(2)	90	90	90	90
β (º)	90.178(2)	90	105.7949(10)	90	90
γ (º)	64.723(2)	90	90	90	90
V (Å^3)	6316.5(3)	2039.00(18)	10444.3(13)	2039.80(4)	20135.2(2)
Z	2	2	8	2	16
Temperature (K)	100(2)	100(2)	150(2)	100(2)	100(2)
Wavelength (Å)	0.71073	0.71073	0.71073	0.71073	0.71073
Calculated density (g.cm^{-3})	1.177	1.300	1.327	1.442	1.341
Absorption coefficient (mm^{-1})	1.87	0.37	2.36	2.88	2.34
Transmission factors (min./max.)	0.701, 1.000	0.530, 1.000	0.223, 0.637	0.894, 0.972	0.520, 1.000
Crystal size (mm^3)	0.22 × 0.02 × 0.01	0.05 × 0.04 × 0.01	0.91 × 0.38 × 0.21	0.04 × 0.04 × 0.01	0.20 × 0.20 × 0.10
θ(max) (°)	27.5	29.9	30.6	27.5	27.5
Reflections measured	132368	14183	80771	92458	118438
Unique reflections	28978	2729	15974	2357	11532
R_{int}	0.090	0.196	0.041	0.033	0.041
Reflections with $F^2 > 2\sigma(F^2)$	20575	1987	13856	2357	10974
Number of parameters	1344	135	628	135	612
R_1 [$F^2 > 2\sigma(F^2)$]	0.062	0.074	0.037	0.023	0.032
wR_2 (all data)	0.124	0.194	0.075	0.070	0.062
GOOF, *S*	1.08	1.04	1.19	1.12	1.28
rgest difference peak and hole (e Å	3.61 and –2.00	0.86 and –1.14	1.32 and –2.35	0.93 and –0.36	0.71 and –0.53

Conflicts of interest

There are no conflicts of interest to declare.

Acknowledgments

CR thanks the Shaanxi Province for the 100 talents award, Northwest University for financial support and the EPSRC for an Overseas travel grant. We also thank the EPSRC National Crystallography Service at

Southampton (UK) and the EPSRC Mass Spectrometry Service, Swansea (UK). K. W and T. X. thank the Chinese Scholarship Council (CSC) for funding.

References

[1] A. Messerschmidt, R. Huber, T. Poulos and K. Weighardt, *Handbook of Metalloproteins*, John Wiley & Sons, New York, 2000.

[2] C. J. Doonan, D. J. Nielsen, P. D. Smith, J. M. White, G. N. George, and C. G. Young, *J. Am. Chem. Soc.*, 2006, **128**, 305–316.

[3] (a) R. H. Holm, *Coord. Chem. Rev*. **1990**, *100*, 183-221. (b) R. H. Holm, *Coord. Chem. Rev*. 2011, **255**, 993-1015.

[4] See for example R. R. Conry and A. A. Tipton, *J. Biol. Inorg. Chem*. 2001, **6**, 359-366.

[5] For reviews, see (a) C. Redshaw, *Coord, Chem. Rev*. 2003, **244**, 45-70. (b) D. H. Homden and C. Redshaw, *Chem. Rev*. 2008, **108**, 5086-5130. (c) A. Arbaoui and C. Redshaw, *Polym. Chem*. 2010**, 1,** 801-826. (d) Coordination Chemistry and Applications of Phenolic Calixarene–metal Complexes. Y. Li, K.-Q. Zhao, C. Redshaw, B. A. Martínez Ortega, A. Y. Nuñez, T. A. Hanna in Patai's Chemistry of Functional Groups. Wiley 2014.

[6] (a) Y. Li, K.-Q. Zhao, C. Feng, M. R. J. Elsegood, T. J. Prior, X. Sun, and C. Redshaw, *Dalton Trans*. 2014, **43**, 13612-13619. (b) W. Yang, Q. -K. Zhao, C. Redshaw, and M. R. J. Elsegood, *Dalton Trans*, 2015, **44**, 13133-13140. (c) Y. Al-Khafaji, T. J. Prior, M. R. J. Elsegood and C. Redshaw, *Catalysts* 2015, **5**, 1928-1947.

[7] Y. Takashima, Y. Nakayama, H. Yasuda and A. Harada, *J. Organomet. Chem*. 2002, **651**, 114-123.

[8] C. Redshaw and S. M. Humphrey, *Polyhedron*, 2006, **25**, 1946-1954.

[9] (a) C. Redshaw, M. J. Walton, M. R. J. Elsegood, T. J. Prior and K. Michiue, *RSC Advances,* 2015, **5**, 89783-89796. (b) Y. Al-Khafaji, X. Sun, T. J. Prior, M. R. J. Elsegood, and C. Redshaw, *Dalton Trans*. 2015, **44**, 12349 – 12356. (c) F. Ge, Y. Dan, Y. Al-Khafaji, T. J. Prior, L. Jiang, M. R. J. Elsegood and C.

Redshaw, *RSC Adv.* 2016, **6**, 4792-4802. (d) J. A. L. Wells, M. L. Seymour, M. Suvova and P. L. Arnold, *Dalton Trans*. 2016, **45**, 16026-16032.

[10] F. Corazza, C. Floriani, A. Chiesi-Villa and C. Guastini, *J. Chem. Soc. Chem. Commun*. 1990, 640-641.

[11] (a) F. Corazza, C. Floriani, A. Chiesi-Villa and C. Rizzoli, *Inorg. Chem*. 1991, **30**, 4465-4468. (b) A. Zanotti-Gerosa, E. Solari, L. Giannini, C. Floriani, A. Chiesi-Villa and C. Rizzoli, *Chem. Commun*. 1996, 119-120.

[12] M. H. Chisholm, K. Folting, W. E. Streib and D. –D. Wu, *Inorg. Chem*. 1999, **38**, 5219-5229.

[13] L. Liu, L. N. Zakharov, J. A. Golen, A. L. Rheingold, W. H. Watson and T. A. Hanna, *Inorg. Chem*. 2006, **45**, 4247-4260.

[14] (a) P. Mongrain, J. Douville, J. Gagnon, M. Drouin, A. Decken, D. Fortin and P.D. Harvey, *Can. J. Chem*. 2004, **82**, 1452-1461. (b) M. Brown and C. Jablonski, *Can. J. Chem*. 2001, **79**, 463-471.

[15] A. Arduini, C. Massera, A. Pochini, A. Secchi and F. Ugozzoli, *New J. Chem*. 2006, **30**, 952-958.

[16] (a) T. A. Hanna, A. K. Ghosh, C. Ibarra, M. A. Mendez-Rojas, A. L. Rheingold and W. H. Watson, *Inorg. Chem*. 2004, **43**, 1511-1516. (b) T. A. Hanna, A. K. Ghosh, C. Ibarra, L. N. Zakharov, A. L. Rheingold and W. H. Watson, *Inorg. Chem*. 2004, **43**, 7567-7569.

[17] W. Clegg, R. J. Errington, P. Kraxner, and C. Redshaw, *Dalton Trans*. 1992, 1431-1438.

[18] See for example G. D. Andreetti, R. Ungaro and A. Pochini, *J. Chem. Soc. Chem. Comm*. 1979, 1005 –1007.

[19] M. H. Chisholm, K. Folting, J. C. Huffman and E. M. Kober, *Inorg. Chem*. 1985, **24**, 241-245

[20] J. Attner and U. Radius, *Chem. Eur. J*. 2001, **7**, 783-790.

[21] (a) V. C. Gibson, C. Redshaw, W. Clegg and M. R. J. Elsegood, *Chem. Comm*. 1995, 2371-2372. (b) G. Guillemot, E. Solari, R. Scopelliti, and C. Floriani, *Organometallics* 2001, **20**, 2446-2448. (c) C. Redshaw and M. R. J. Elsegood, *Eur. J. Inorg. Chem.* 2003, 2071-2074. (d) U. Radius, and J. Attner, *Inorg. Chem*. 2004, **43**, 8587-8599. (e) C. Redshaw, D. Homden, D. L. Hughes, J. A. Wright and M. R. J. Elsegood, *Dalton Trans*. 2009, 1231-1242.

[22] Y. Mahha, A. Atlamsani, J. –C. Blais, M. Tessier, J. –M. Brégeault and L. Salles, *J. Mol. Cat. A. Chem*. 2005, **234**, 63-73.

[23] M. Bouyahya and R. Duchateau, *Macromolecules*, 2014, **47**, 517-524.

[24] L. H. Tang, E. P. Wasserman, D. R. Neithamer, R. D. Krystosek, Y. Cheng, P. C. Price, Y. Y. He and T. J. Emge, *Macromolecules*, 2008, **41**, 7306-7515.

[25] (a) G. M. Sheldrick, *Acta Cryst*. 2015, **A71**, 3-8. (b) G. M. Sheldrick, *Acta Cryst*. 2015, **C71**, 3-8.